Study of a mesoscale anticyclonic eddy in the western part of the Gulf of Lion.

Z. Y. Hu [a,*], A. A. Petrenko [a], A. M. Doglioli [a], I. Dekeyser [a]

[a] *Université de la Méditerranée - Aix Marseille II, CNRS, Laboratoire d'Océanographie Physique et Biogéochimique, UMR 6535, OSU/Centre d'Océanologie de Marseille, Campus de Luminy case 901, 13288 Marseille Cedex 9, France.*

Abstract

Acoustic Doppler Current Profiler (ADCP) and Expendable Bathy Thermograph (XBT) data were collected during the Latex08 cruise (September 1 - 5, 2008) throughout the western part of the gulf of Lion. These data, combined with Sea Surface Temperature (SST) satellite images and Lagrangian drifter trajectories, show the presence of an intense anticyclonic eddy in the western part of the gulf of Lion. The eddy is elliptic in shape and the estimated radii are 21.5 (15.5) km for its major (minor) axis. The vertical extent of the eddy reached about 35 m depth and was limited by the bottom of the seasonal mixed layer. The eddy interacts with the Northern Current at the end of the cruise, maybe leading to its deformation. Moreover complementary drifter data suggest that this anticyclonic eddy was already present at the beginning of August 2008. Hence the eddy lasted around 50 days in the same region. In light of previous numerical study, some hypotheses about the formation and behaviour of the eddy are also discussed.

Key words: mesoscale eddies; Gulf of Lion; northwestern Mediterranean Sea; LATEX project

1 Introduction

Oceanic eddies may have an important impact on transfer and redistribution of heat, energy and matter. Several studies have previously focused on mesoscale eddies and their influences on biogeochemical distributions (e.g. Garon et al.,

* Corresponding author.
Email address: ziyuan.hu@univmed.fr (Z. Y. Hu).

2001; Taupier-Letage et al., 2003; McGillicuddy et al., 2007; Benitez-Nelson et al., 2007). Nevertheless, questions remain, particularly in coastal waters where dynamical processes are very complex and fluxes of nutrients and sediments are high.

The Gulf of Lion (hereafter GoL) is a large continental margin with a semi-circle shape located in the northwestern Mediterranean Sea (Fig. 1). The hydrodynamics of the GoL are complex and highly variable, as described by Millot (1990). Three main forcings coexist:
i) strong continental winds: the Mistral (northerly) and the Tramontane (north-westerly, sometimes westerly). They are cold and dry and can generate strong upwellings and downwellings along the entire coast of the GoL (Millot, 1979);
ii) a quasi-geostrophic alongslope current: the Northern Current (hereafter NC). It is the northern part of the cyclonic gyre occurring in the western Mediterranean basin. The NC flows along the continental slope from the Ligurian Sea to the Catalan Sea (Millot, 1990, 1999). As a first approximation, the NC can be considered in geostrophic balance, acting as a dynamical barrier for coastal waters. Nevertheless, several studies have demonstrated the presence of transient ageostrophic processes (Albérola et al., 1995; Sammari et al., 1995; Petrenko, 2003);
iii) important fresh waters inputs, bringing nutrients that enhance primary productivity on the shelf (e.g. Minas and Minas, 1989; Ludwig et al., 2009). The Rhone river on the north-eastern part of the gulf delivers about 80% of the total riverine water inputs and constitutes the main fresh water source of the GoL. The plume extension of the Rhone can extend offshore towards the southwest part of the GoL under certain meteorological conditions (Estournel et al., 1997).

Previous *in situ* studies suggested the presence of an anticyclonic circulation in the western part of the GoL, in September during stratified conditions (Millot, 1979, 1982). Estournel et al. (2003) have also shown with numerical modelling that an anticyclonic circulation can be present in this region in winter. These coastal eddies could potentially be influenced by the Rhone distal plume which could bring nutrients and phytoplankton inside the eddy. Numerical modelling suggests that the eddy can interact with the NC (Hu et al., 2009). Such interactions, whether with the river plume or the neighboring current, indicate that these eddy structures could play an important role in the coastal-offshore transport of nutrients and phytoplankton, as well as heat and energy. To our knowledge, no experimental studies have been dedicated on the study of the eddy dynamics in this area since the early hypothesis of Millot (1979, 1982) cited earlier.

The main objective of this paper is to investigate the dynamical characteristics of an anticyclonic eddy observed during the Latex08 cruise, adding cruise data to the previous numerical study by Hu et al. (2009), to better under-

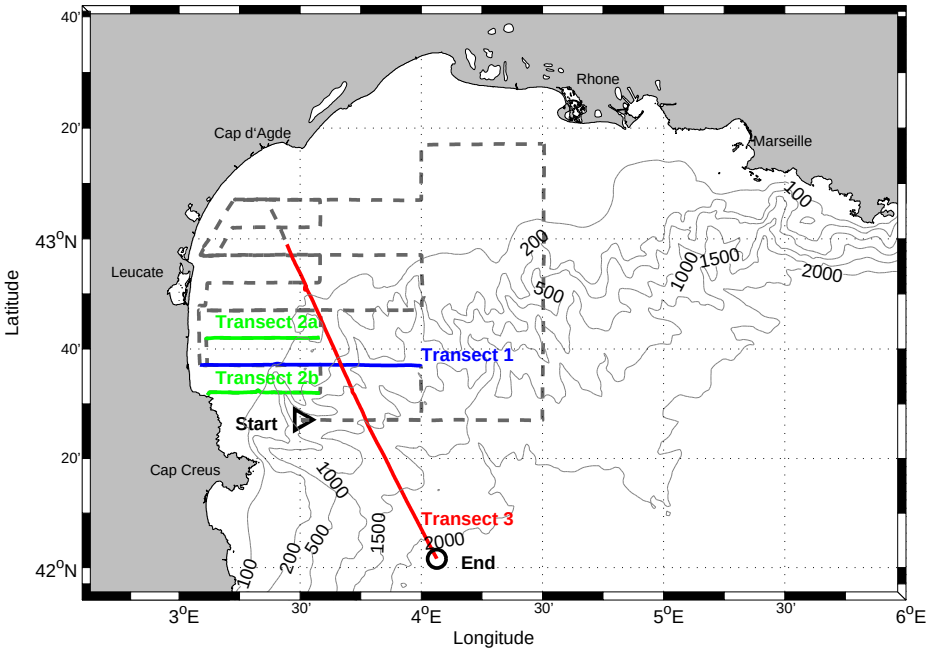

Fig. 1. Map of the Gulf of Lion with the complete Latex08 ship trajectory. The transects used in the study are overlined in colors. Isobaths at 100, 200, 500, 1000, 1500 and 2000 m are plotted with thin lines.

stand coastal mesoscale structures. The material and methods used in the experiment are described in Section 2 and the results are presented in Section 3. Eddy features and the possible mechanisms of its generation and its behaviour are discussed in Section 4. In the final section, we summarize the main results and briefly describe the perspective work.

2 Material and methods

The strategy of the LATEX project combines use of data from satellite observation, *in situ* measurements and numerical modelling. The Latex08 cruise was conducted from September 1 to 5, 2008 on board the RV *Téthys II*. The data collected during Latex08 came from satellite, ship-based and drifters observations.

A few days prior to the beginning of the Latex08 cruise, some eddy-like features appeared in the study region on SST satellite images provided by Météo-France (data not shown). Specifically, an eddy feature was present in the coastal waters east of Leucate. During the cruise, SST images were e-mailed to the RV *Téthys II* to help us track the eddy. Unfortunately, at the beginning of the cruise extensive cloud coverage limited our ability to determine the optimal sampling region for the eddy. Thus, based on numerical modelling

results (Hu et al., 2009), we decided to start the sampling by doing a 10nm spaced radiator throughout the western region (Fig. 1).

Because of the complexity of the measured currents, we pursued with a reduced 5nm spaced radiator closer to the coast. Then, the image of September 2 showed us the presence of an eddy-like feature close to the continental slope (Fig. 2). Hence, at the end of the small radiator, we decided to cross through it diagonally from the northwest to the southeast direction (Transect 3 in Fig. 1). However, later in the cruise, the SST image was again disturbed by both clouds and the cold signature of surface waters upwelled by the Tramontane. Hence, the image on September 2 is the only informative image available during the cruise.

A ship-mounted VMBB-150 kHz ADCP, merged at 3 m below the water surface, was used to measure current velocity. Following Petrenko et al. (2005), the ADCP configuration used during the cruise was: 60 cells of 4 m depth, an ensemble average of 1 min and bottom tracking when possible. Consequently, the depth range of current data covers 11 to 243 m. The software for ADCP data analysis was provided by the French INSU (*Institut National des Sciences de l'Univers*) technical division. The measured ADCP horizontal currents were analyzed in near-real time during the entire cruise.

Since the sea state did not allow the use of the SeaBird SBE 19 CTD we had on board, temperature profiles were obtained by using XBTs. The reader can refer to Fig. 3 for the location of the XBT profile launched on September 5 at 04:32 PM UTC. Two satellite-tracked drifters, equipped with a 6 m long holey-sock drogue, extending between 12m and 18m, were deployed in the eddy to track the fluid motion of the eddy at 15 m depth (Fig. 2, Fig. 3). Drifter positions are provided by Argos system in quasi-real time.

3 Results

The eddy is clearly apparent in ADCP, drifters and SST data. For the sake of clarity, we show the SST image in Fig. 2 and the ADCP measurements in Fig. 3. The drifters trajectories were added on both figures in order to obtain a synoptic view of the sampled eddy. Then, XBT data are combined with a vertical section of the ADCP data.

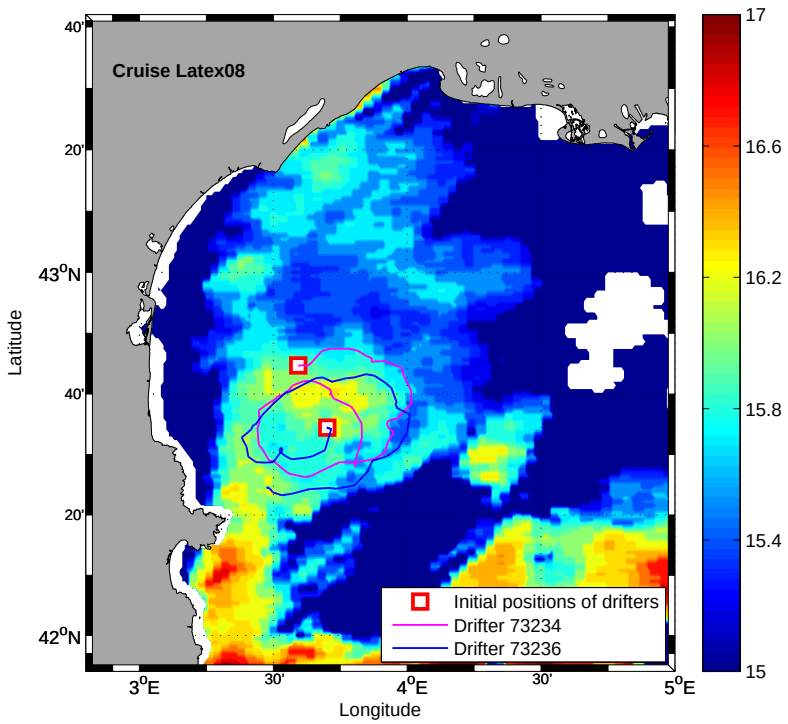

Fig. 2. SST satellite image (Sept. 2) (data from Météo-France) and drifters trajectories (Sept. 5 - 11).

3.1 ADCP data

ADCP horizontal current velocity vectors at 15 m depth (corresponding to the same depth as the drifter measurements) for Transects 1, 2a, 2b and 3 clearly revealed the clockwise motion field associated with an anticyclonic eddy feature (Fig. 3). In Transects 1 and 3, the current speed increases gradually before reaching a peak and then decays until reaching its minimum values near the transect crossing, and increases again on the other side in the opposite direction. Transects 2a and 2b did not cross the eddy but showed the continuity of the anticyclonic circulation. Maximum velocity magnitude inside this eddy is about 0.6 ms^{-1}.

In order to accurately locate the geometric position of the eddy center for each transect, we followed the method described in Nencioli et al. (2008). A square area 30 $\times$ 30 km (colored squares in Fig. 4) was defined around the minimum velocity zone of each transect and then was divided into a grid of 30 $\times$ 30 points. Then, each point of that grid was tested as a possible location for the center of the eddy, decomposing ADCP velocities into tangential and radial components relative to the tested point. At all depths the center of the eddy was defined as the grid point for which the mean absolute value of tangential (radial) component was maximal (minimal). For Transect 1 (3)

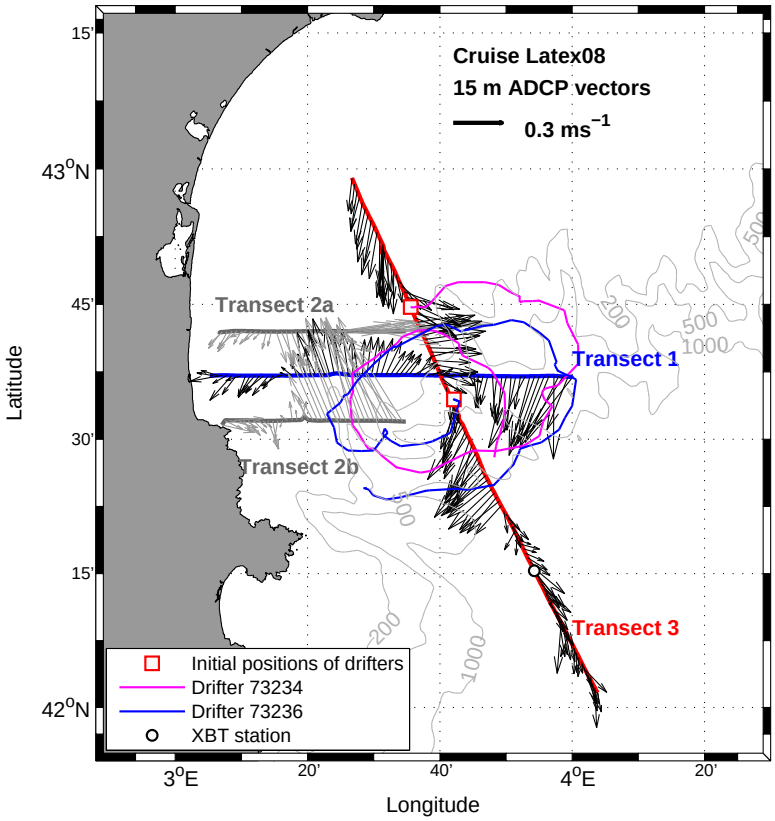

Fig. 3. ADCP current vectors (plotted every 4 minutes) in the upper layer (15-m) for Transects 1 (Sept. 1), 2a and 2b (Sept. 3) and 3 (Sept. 5); blue and magenta lines represent the two drifters trajectories (Sept. 5 - 11). Isobaths at 200, 500 and 1000 m are plotted with thin lines.

the above velocity decomposition was performed on the nearest 200 (155) records of ADCP measurements (black vectors in Fig. 4a and b). We used only these latter vectors in order that the estimation of the center location not be affected by the peripheral flow of the eddy which is more perturbed by the outer velocity field. We tested the sensivity to the numbers of vectors used (data not shown). The present result is considered to be the best estimation since it is least influenced by surrounding current fields. From now on, we choose to continue the analysis using the eddy centers determined with the tangential components of ADCP velocities since tangential velocities within the eddy are usually much higher in magnitude than radial velocities and hence are less sensitive to the variations due to background noise. Fig. 4 shows the estimated center positions for Transect 1 (a) and Transect 3 (b) at 15 m depth. The estimated location of the eddy center derived from ADCP vectors at 15 m depth was 42°36′N, 3°40′W (42°37′N, 3°43′W) for Transect 1 by using the tangential (radial) components; and 42°34′N, 3°37′W (42°33′N, 3°37′W) for Transect 3, with an incertitude of about 1 km which is the size of the grid within the square area. The differences between the two methods

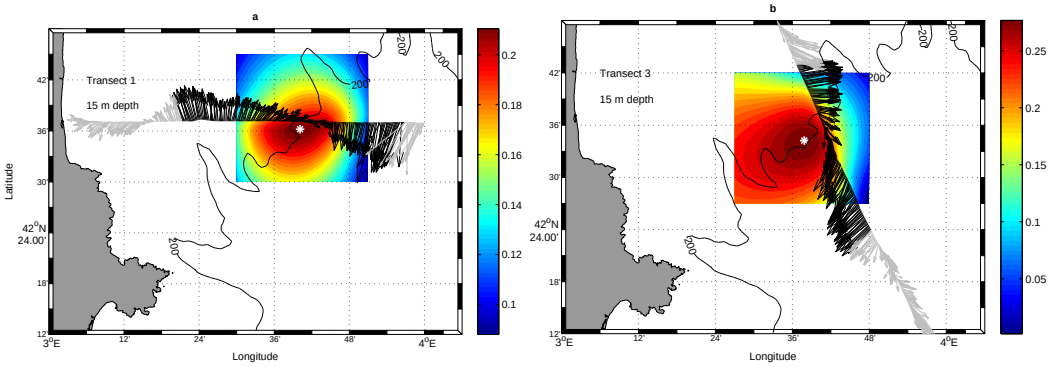

Fig. 4. Estimated center location of anticyclonic eddy (white asterisk) for Transect 1 (left) and Transect 3 (right) at 15 m depth. Tangential components of the black vectors were computed for each point within the grids. For each transect, the center of the eddy was defined as the point for which the mean absolute value of tangential velocity was maximal. The contours in the square areas indicate values of equal mean absolute tangential velocity (ms^{-1}). Isobath at 200 m is plotted with black line.

in the present case are relatively small. Analysis shows that the survey line of Transect 1 was very close to the eddy's center while Transect 3 was a few km to the east. The estimated position of the eddy center at 15 m depth moved 5 km southwest during the 4 days separating these two transects. The resulting drifting velocity of the eddy is 0.01 ms^{-1}. Moreover, we estimated the variation of the eddy center location with depth and we obtained $2'$ of latitude and $3'$ of longitude for Transect 1 and $1'$ of latitude and $1'$ of longitude for Transect 3.

In Fig. 5 we plotted the radial and tangential velocities at 15 m depth computed for both Transects 1 and 3 versus the radial distance from the estimated eddy center. The blue dots in the figures correspond to the data from the section before crossing the center of the eddy (western part for Transect 1 and northern part for Transect 3) while the red ones represent the data from the section after crossing the center. The eddy center is at a distance of 1.7 km from Transect 1, and at about 5 km from Transect 3 (Fig. 5a and b). For each transect, the values of radial velocities are near zero within the eddy and become greater with radial distance due to the influence of the outer circulation field (Fig. 5a1 and a2). The tangential velocities are smallest near the eddy center. During Transect 1, they increased roughly linearly outward with radial distance until their maximum magnitude (V_{max}), and then decayed (Fig. 5b1). However this linearity was not so clear for Transect 3, since Transect 3 was further away from the eddy center (Fig. 5b2) than Transect 1. Furthermore, for both transects, the tangential velocities of the two radial sections reached their maximum value at different distances R_{max} from the center. R_{max} equals 20 (23) km for the eastern(western) section of Transect 1; R_{max} equals 14 (17) km for the northern(southern) section of Transect 3.

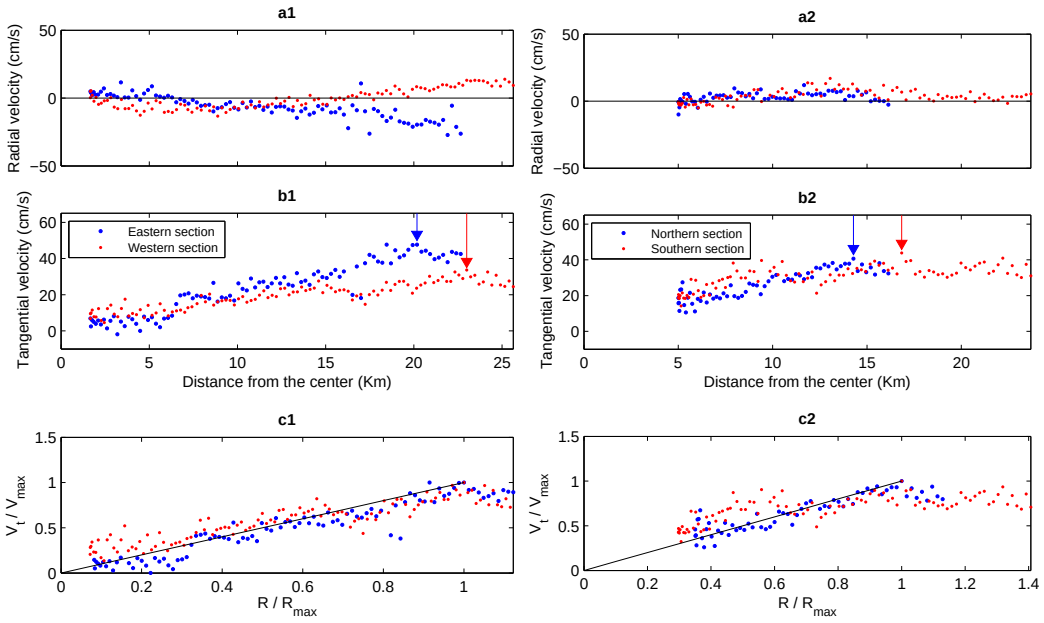

Fig. 5. Distribution of (a) radial and (b) tangential velocities with respect to radial distance from the center; (c) distribution of normalized tangential velocity with respect to normalized radial distance for both Transect 1 (left column) and Transect 3 (right column). Arrows in (b) indicate the locations of maximum velocity magnitude for two sections; the solid lines in (c) indicate values of equal angular velocity (V_{max}/R_{max}).

The fact that the maximum tangential magnitudes of both radial sections were different and were reached at different radial distances from the center, suggests that the sampled anticyclonic eddy was asymmetric. Following Olson (1980), angular velocity can be computed as the tangential velocity (V_t) divided by the radial distance (R) from the determined center of the eddy. In Fig. 5c, we plotted the normalized tangential velocities (V_t/V_{max}) against the normalized radial distances (R/R_{max}). The solid lines in the Fig. 5c thus represent a constant value of the angular velocity (V_{max}/R_{max}). The part of the eddy with a constant angular velocity is roughly considered as a solid body in which the rotation of the eddy is isolated from the surrounding waters. This confirms that the solid body rotation is included in the elliptical shape whose dimensions are detailed previously.

3.2 Drifter data

Drifter trajectories obtained six days after their launch during the Latex08 cruise are displayed in Fig. 2 and Fig. 3. The two drifters were deployed on September 5. Drifter N°73234 was deployed on Transect 3 near the northern outer edge of the eddy and drifter N°73236 was deployed at the center of the

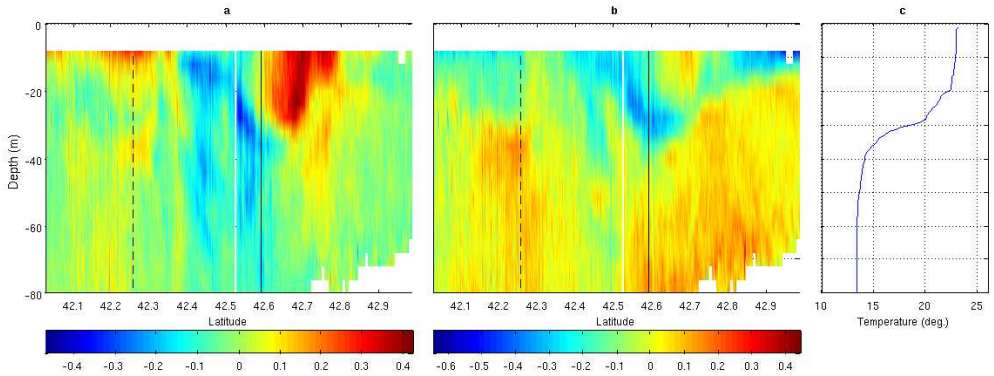

Fig. 6. Vertical sections (depth vs. latitude) of the horizontal currents (colors; ms^{-1}) for Transect 3: a) the observed west-east component (eastward, positive); b): the observed south-north component (northward, positive); c): the temperature profile measured by XBT at the location marked by dotted line; the solid line indicates the nearest position to the estimated eddy center using 15 m ADCP data.

eddy, according to the ADCP data. Both drifters made one full loop around the eddy in about 5 days. The trajectories of these two drifters followed the outer edge of the eddy indicated in the SST satellite image, and clearly revealed the well developed warm-core anticyclonic feature of the eddy (Fig. 2). These trajectories further confirmed the asymmetric nature of the eddy and suggested that it has an elliptical shape with its major axis being oriented southwest (SW) to northeast (NE). The time-averaged translational velocity of each drifter was calculated as the distance covered by the drifter divided by the corresponding time interval. This velocity can be considered as the drifter-based tangential velocity $V_t^{Drifter}$ of the eddy at its outer edge and at 15 m depth. For the drifter N°73234 (N°73236) we obtained $V_t^{Drifter} = 0.48$ (0.41) ms^{-1}. Moreover, we considered the distance between the two drifter positions near the endpoints of the SW-NE (NW-SE) axis as the major (minor) diameter of the elliptical eddy. Then, the estimated eddy major (minor) radii $R^{Drifter}$ are equal to 25 (18) km for the drifter N°73234 and 24 (17) km for the drifter N°73236.

3.3 Vertical profiles

The vertical sections of the ADCP derived east-west (U) and south-north (V) current components show the whole eddy extension (Fig. 6a and b respectively). U (V) is defined as positive when the current is eastward (northward). The solid lines indicate the projection, on the transect, of the estimated eddy center using the 15 m ADCP data (section 3.1). Two areas with opposite directions on both sides of the eddy center and with relatively high value in magnitude, represent a typical eddy. Here the northern section (Fig. 6a) of the eddy reveals a clear red (positive) spot since the current vectors - in this

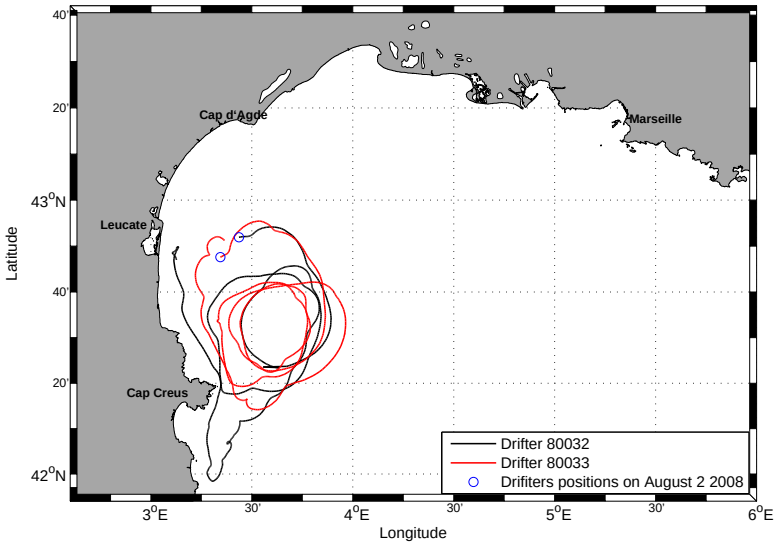

Fig. 7. Additional Argos drifters trajectories (August 2 - 19, 2008).

section - are almost eastward. The eddy signature is less obvious in the southern part. This reinforces the observation that the eddy is not circular. Vertical current distribution shows that the horizontal extent of the eddy decreases with depth increasing, and that there is no eddy at depths deeper than 35 m. The temperature profile measured with an XBT at the location marked by the dotted line is shown in Fig. 6c. The temperature is about 23°C at the surface and decreases progressively with depth to the value of 13.4°C at about 60 m depth, which is the typical temperature of the Modified Atlantic Water (MAW) in this area (Albérola and Millot, 2003). The marked thermocline depth is about 35 m, suggesting that the vertical extent of the anticyclonic feature was limited by the bottom of the mixed layer.

4 Discussion

The combined analysis of the ADCP and drifter data revealed that the eddy was approximately elliptical and elongated along the southwest to northeast direction. In order to fix a unique value for the two radii of the eddy solid body rotation, we averaged the values of ADCP-based R_{max} and obtained a major radius of 21.5±1.5 km and a minor radius of 15.5±1.5 km. These values are slightly smaller than the radii estimated from drifter trajectories. In fact, averaging the values for the two drifters N°73234 and N°73236, we obtained a major radius of 24.5±0.5 km and a minor radius of 17.5±0.5 km. We explain these differences by the fact that both drifters looped in the outer edge of the eddy, just outside of the solid body rotation, as suggested by their $V_t^{Drifter}$ smaller than V_{max} and by the overlappings of the drifter trajectories with ADCP vectors (Fig. 3) and SST contours (Fig. 2). Moreover, the eddy

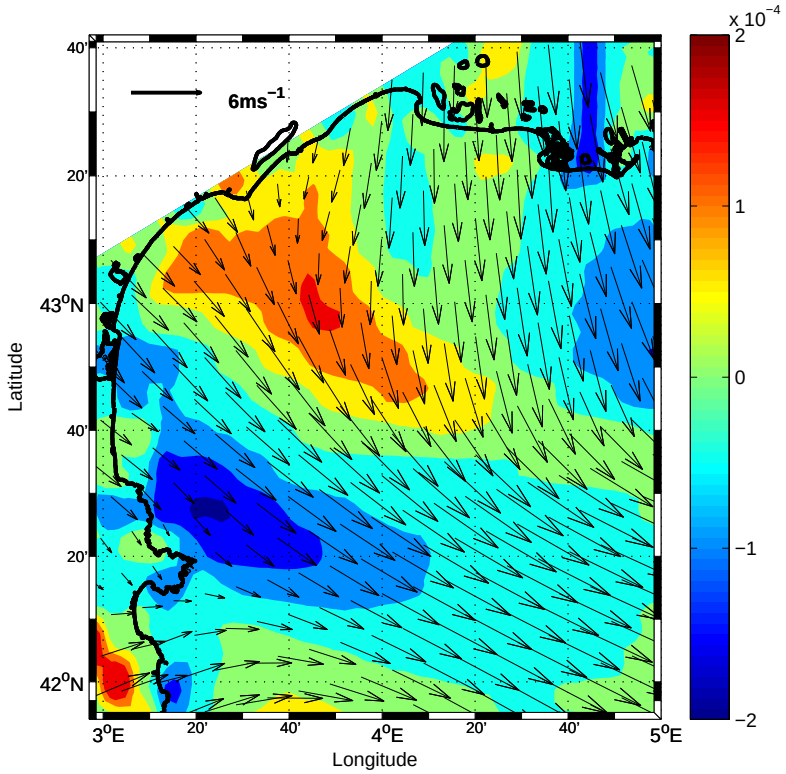

Fig. 8. Wind vectors at 10 m altitude in ms^{-1} and wind stress curl in s^{-1} on September 2, 2008. Results from the Météo-France ALADIN meteorological model.

radius values agree with our previous study. Indeed, in Hu et al. (2009), a numerical eddy simulated for the year 2001 had a time-averaged area during its life duration of about 1193 km^2. Assuming a circular shape for the eddy, the radius corresponding to this area value is hence about 20 km. These values of the estimated radius of the eddy are comparable with the Rossby radius of this area, suggested to be 15 km by Grilli and Pinardi (1998). The magnitude and direction of current vectors derived from drifters trajectories were in a good agreement with the ADCP velocities at 15 m depth. The maximum velocity within the eddy is 0.6 ms^{-1}, indicating that it is an intense coastal eddy. Compared to the position of the eddy simulated for the year 2001 (Hu et al., 2009), the eddy observed during the Latex08 cruise in 2008 is farther offshore and more to the south.

In order to estimate the life duration of the Latex08 eddy, we need more information. On one hand, on July 21, 2008, two Argos drifters with an anchor depth of 15 m were launched in the GoL (drifter data can be found at http://www.coriolis.eu.org/default.htm as numbers 80032 and 80033). Both drifters were entrained simultaneously (August 2) into an anticyclonic eddy, which had a similar shape and was located in the same position as the one sampled during the experiment Latex08. The drifters spun up nearly four times in the eddy until the middle of August (Fig. 7). Then, the two Argos

drifters moved northward along the coast. In addition, in the SST satellite images without cloud coverage, a similar eddy-like structure was observed in the western part of the GoL in August (data not shown). On the other hand, Hu et al. (2009) showed that, in the same region, an anticyclonic eddy persisted for more than a month in 2001 (56 days) both in simulation results and in satellite observations. Hence, it is quite possible that the eddy evidenced in August 2008 by the drifters N°80032 and N°80033 was the same as the one sampled during the Latex08 cruise. Since the drifter trajectories in the beginning of August show that the eddy was already well developed, the 'birth' of the eddy is assumed to be at least one to two weeks earlier, between the middle and the end of July. The life of this eddy is thus reasonably assumed to be at least 50 - 60 days.

In the numerical experiments of Hu et al. (2009), the 'death' of the eddy in 2001 happened in the middle of August when the anticyclonic eddy approached the NC and interacted with it. Such interaction was considered fatal to the eddy and brought its collapse. The present analysis of the ADCP data shows that R_{max} on the southern section of Transect 3 is greater than R_{max} on the northern section and that the maximum of current velocity along Transect 3 is also found on the southern section. Hence, we suppose that, at the end of the cruise, this anticyclonic eddy interacted at its southeastern side with the NC and was stretched and accelerated by it, as along Transect 1 and 3, where the current stayed intense with depth. Instead, the amplitude of the current vectors along Transect 2b decreased quickly with depth, were halved at 23 m depth, and became even weaker below 31 m (data not shown) probably due to a local wind effect. Whether these hypotheses are true or not remains an open question until future modelling experiments provide more information. Unfortunately, no available data can help us verify whether or not the eddy still existed after this interaction with the NC.

Regarding the formation of such an anticyclonic eddy, we consider the following mechanism, based on the work by Millot (1982). During a Tramontane event, a southeastward wind-driven current appears south of Cap d'Agde. Coastal waters pushed offshore are partly compensated by upwelled waters. The deficit part is compensated by a northward coastal jet near Leucate. Under the Coriolis effect, the wind-driven offshore current shifts southwestly onshore to Cap Creus. There, it joins the beginning of the northward current along the coast and as such, closes the loop forming the anticyclonic circulation. Once the eddy is generated, we think, based on model simulations, that it can survive longer than a month. Different mechanisms probably intervene as fueling processes maintaining this eddy. We propose here two mechanisms. The first one is the direct effect of wind stress curl on the west part of the GoL. The wind time series (data from the ALADIN meteorological model, provided by Météo-France) over the GoL show that, near the Roussillon coast, the gradients in the wind velocity fields favor an anticyclonic wind stress curl, such as

on September 2, 2008 (Fig. 8). Transmission of the anticyclonic wind momentum to the sea surface could feed the anticyclonic vorticity of the eddy after its generation. The second potential fueling mechanism is the baroclinic instability of the NC. Indeed, during the MATER HFF experiment, Flexas et al. (2002) observed from satellite SST images that, when the NC propagates to the western part of the GoL, anticyclonic motions due to baroclinic instability may occur on the inner edge of the NC. The possible mechanisms for this baroclinic instability may result from diverse factors such as the wind stress, topographic irregularities (canyons) and along-shelf variations, etc. Otherwise, in the numerical experiments, Hu et al. (2009) also showed the appearance of anticyclonic features on the inner edge of the NC.

The estimated drifting velocity of 0.01 ms^{-1} of the observed eddy is 10 times smaller than the previously reported drifting velocity of eddies in the studied region. In Allou et al. (2010), the eddies located in the eastern part of the GoL shifted at 0.1-0.2 ms^{-1}; while in Rubio et al. (2005), the eddies located downstream of the GoL shifted at 9 km/day (i.e. 0.1 ms^{-1}). In these two latter cases, the eddies are instabilities of the NC meanders in the eastern part of the GoL as we mentioned earlier, and are (partially) advected by the NC. Hence, the drifting velocities of these eddies have values which are comparable to the one of the NC which propagates at speeds of 10-20 km/day (i.e. 0.1-0.2 ms^{-1}), as documented by Crépon et al. (1982); Millot (1999); Sammari et al. (1995); Petrenko et al. (2005). Ginzburg et al. (2002) proposed a value of 0.043 ms^{-1} for eddy's drifting velocity in the shelf area of the Black Sea where hydrodynamic conditions are similar to the NWM (the Rossby radius of deformation in the Black Sea is of the order of 20-30 km, according to Stanev et al. (2002); Stanev (2005)).

5 Conclusions and Perspectives

During the Latex08 cruise, a coastal mesoscale anticyclonic eddy was sampled in the western part of the GoL. SST satellite images suggested presence of a structure at the surface, while ADCP current data not only confirmed the presence of the eddy, but also gave us the dynamic characteristics of the eddy structure. Furthermore, the time series of the fluid motion associated with the eddy derived from drifter data provided complementary information on the eddy characteristics. From these data, we have greatly increased our knowledge on these eddy features, which was previously mainly based on numerical modellingf. The studied anticyclonic eddy may have lasted 50 - 60 days. It was characterized by an elliptical shape with radius about 21.5 (15.5) km for its major (minor) axis and by a maximum tangential velocity of about 0.6 ms^{-1}. The vertical extent of the eddy has been estimated to be 35 m, which was also the bottom depth of the thermocline. Analysis results suggested that the eddy

interacted with the NC at the end of the cruise. The generation of the eddy in this region is considered to be due to an enclosed anticyclonic circulation linked to an upwelling phenomena. Moreover the eddy is suspected to be fueled by two additional processes: the direct wind stress curl and anticyclonic baroclinic instabilities of the NC.

Ongoing numerical modelling work focuses on a 10-year (2001-2010) simulation with the same model configuration discussed in Hu et al. (2009). The numerical modelling may allow us to verify the assumption on the eddy's life duration; to explain the difference in the eddies' locations in 2001 and 2008; to study the eddy's evolution throughout its lifetime and to investigate whether the eddy dies after its interaction with the NC at the beginning of September 2008. During the second cruise of the LATEX project (Latex09, August 25-30, 2009), three Eulerian ADCPs were moored to constitute an on-offshore eddy-crossing transect between the coast and the area where the eddy has been observed, and will provide us a one-year time series (August 2009 - September 2010) of horizontal current measurements through the water column. These data will allow us to systematically evaluate the circulation in this key area where eddies regularly form, in order to detect the presence of eddy structures and, furthermore, to study the phenomena associated with the wind variation near the coast. Such data, as well as meteorological data and future numerical modelling work, will help us test our hypotheses regarding eddy generation and fueling. The third LATEX project cruise (Latex10, planned for September 6-30, 2010) will add, to the strategy used in the present work, an inert tracer release and glider measurements with the objective of better understanding the remaining open questions about the coupled physical and biogeochemical dynamics at mesoscale and their role in the transfers between the GoL coastal zone and the northwestern Mediterranean open ocean.

Acknowledgements

The cruise and the LATEX projet are supported by the programs LEFE/IDAO and LEFE/CYBER of the INSU-Institut National des Sciences de l'Univers and by the Region PACA-Provence Alpes Côte d'Azur. The SST satellite and meteorological data were supplied by Météo-France. We are warmly grateful to the crews of the R/V *Téthys II*, Gilles Rougier, Frédéric Diaz and Stéphane Blain for their assistance. We thank Francesco Nencioli for providing the Matlab routines for ADCP analysis. We also thank G. Eldin (from IRD), V. Dutreuil (from INSU) for their suggestions in ADCP data analysis and Pierre Garreau (from IFREMER) for providing us additional drifter data. Z.Y. Hu is financed by a MENRT Ph.D. grant.

References

Albérola, C., Millot, C., 2003. Circulation in the French Mediterranean coastal zone near Marseilles: the influence of the wind and the Northern Current. Cont. Shelf Res. 23, 587–610.

Albérola, C., Millot, C., Font, J., 1995. On the seasonal and mesoscale variabilities of the Northern Current during the PRIMO-0 experiment in the western Mediterranean Sea. Oceanol. Acta 18, 163–192.

Allou, A., Forget, P., Devenon, J., 2010. Submesoscale vortex structures at the entrance of the Gulf of Lions in the Northwestern Mediterranean Sea. Cont. Shelf Res. 30 (7), 724 – 732.

Benitez-Nelson, C. R., Bidigare, R. R., Dickey, T. D., Landry, M. R., Leonard, C. L., Brown, S. L., Nencioli, F., Rii, Y. M., Maiti, K., Becker, J. W., Bibby, T. S., Black, W., Cai, W. J., Carlson, C. A., Chen, F., Kuwahara, V. S., Mahaffey, C., McAndrew, P. M., Quay, P. D., Rappé, M. S., Selph, K. E., Simmons, M. P., Yang, E. J., 2007. Mesoscale Eddies Drive Increased Silica Export in the Subtropical Pacific Ocean. Science 316 (5827), 1017–1021.

Crépon, M., Wald, L., Monget, M., 1982. Low-frequency waves in the ligurian sea during december 1977. J. Geophys. Res. 87, 595 – 600.

Estournel, C., Durrieu de Madron, X., Marsaleix, P., Auclair, F., Julliand, C., Vehil, R., 2003. Observation and modeling of the winter coastal oceanic circulation in the Gulf of Lions under wind conditions influenced by the continental orography (FETCH experiment). J. Geophys. Res. 108 (C3), 7–18.

Estournel, C., Kondrachoff, V., Marsaleix, P., Vehil, R., 1997. The plume of the Rhône: numerical simulation and remote sensing. Cont. Shelf Res. 17 (8), 899 – 924.

Flexas, M., M., Durrieu de Madron, X., Garcia, M. A., Canals, M., Arnau, P., 2002. Flow variability in the Gulf of Lions during the MATER HFF experiment (March-May 1997). J. Mar. Sys. 33-34, 197 – 214.

Garon, V. C., Oschlies, A., Doney, S. C., McGillicuddy, D., Waniek, J., 2001. The role of mesoscale variability on plankton dynamics in the north atlantic. Deep-Sea Res. II 48 (10), 2199 – 2226.

Ginzburg, A. I., Kostianoy, A. G., Krivosheya, V. G., Nezlin, N. P., Soloviev, D. M., Stanichny, S. V., Yakubenko, V. G., 2002. Mesoscale eddies and related processes in the northeastern black sea. J. Mar. Sys. 32 (1-3), 71 – 90.

Grilli, F., Pinardi, N., 1998. The computation of Rossby radii dynamical processes of deformation for the Mediterranean Sea. MTP News 6, 4.

Hu, Z. Y., Doglioli, A. M. Petrenko, A. A., Marsaleix, P., Dekeyser, I., 2009. Numerical simulations of eddies in the Gulf of Lion. Ocean Model. 28 (4), 203 – 208.

Ludwig, W., Dumont, E., Meybeck, M., Heussner, S., 2009. River discharges of water and nutrients to the Mediterranean and Black Sea: Major drivers for ecosystem changes during past and future decades? Prog. Oceanogr.

80 (3-4), 199–217.
McGillicuddy, D.J., J., Anderson, L. A., Bates, N. R., Bibby, T., Buesseler, K. O., Carlson, C. A., Davis, C. S., Ewart, C., Falkowski, P. G., Goldthwait, S. A., Hansell, D. A., Jenkins, W. J., Johnson, R., Kosnyrev, V. K., Ledwell, J. R., Li, Q. P., Siegel, D. A., Steinberg, D. K., 2007. Eddy/Wind Interactions Stimulate Extraordinary Mid-Ocean Plankton Blooms. Science 316 (5827), 1021–1026.
Millot, C., 1979. Wind induced upwellings in the Gulf of Lions. Oceanol. Acta 2, 261–274.
Millot, C., 1982. Analysis of upwelling in the Gulf of Lions 34, 143–153.
Millot, C., 1990. The Gulf of Lions' hydrodynamics. Cont. Shelf Res. 10, 885–894.
Millot, C., 1999. Circulation in the Western Mediterranean Sea. J. Mar. Sys. 20, 423–442.
Minas, M., Minas, H., 1989. Primary production in the Gulf of Lions with considerations to the Rhône River input. Water Pollution Research Reports 32 (5), 112–125.
Nencioli, F., Kuwahara, V. S., Dickey, T. D., Rii, Y. M., Bidigare, R. R., 2008. Physical dynamics and biological implications of a mesoscale eddy in the lee of Hawaii: Cyclone Opal observations during E-Flux III. Deep-Sea Res. II 55, 1252–1274.
Olson, D., 1980. The Physical Oceanography of Two Rings Observed by the Cyclonic Ring Experiment. Part II: Dynamics. J. Phys. Oceanogr. 10, 514–528.
Petrenko, A. A., 2003. Variability of circulation features in the Gulf of Lion NW Mediterranean Sea. Importance of inertial currents. Oceanol. Acta 26, 323–338.
Petrenko, A. A., Leredde, Y., Marsaleix, P., 2005. Circulation in a stratified and wind-forced Gulf of Lions, NW Mediterranean Sea: in situ and modeling data. Cont. Shelf Res. 25, 7–27.
Rubio, A., Arnau, P., Espino, M., Flexas, M., Jordà, G., Salat, J., Puigdefàbregas, J., S.-Arcilla, A., 2005. A field study of the behaviour of an anticyclonic eddy on the Catalan continental shelf (NW Mediterranean). Prog. Oceanogr. 66 (2-4), 142–156.
Sammari, C., Millot, C., Prieur, L., 1995. Aspects of the seasonal and mesoscale variabilities of the Northern Current inferred from the PROLIG-2 and PROS-6 experiments. Deep-Sea Res. I 42, 893–917.
Stanev, E., 2005. Understanding black sea dynamics: An overview of recent numerical modeling. Oceanography. 18, 56–75.
Stanev, E. V., Beckers, J. M., Lancelot, C., Staneva, J. V., Traon, P. Y. L., Peneva, E. L., Gregoire, M., 2002. Coastal-open ocean exchange in the black sea: Observations and modelling. Estuarine, Coastal Shelf Science. 54 (3), 601 – 620.
Taupier-Letage, I., Puillat, I., Millot, C., Raimbault, P., 2003. Biological re-

sponse to mesoscale eddies in the algerian basin. J. Geophys. Res. 108, 3245.

List of Figures

Contents